GEOLOGICA CARPATHICA, 55, 3, BRATISLAVA, JUNE 2004
251–260

LITHOLOGICAL AND MAGNETOSTRATIGRAPHIC CORRELATION OF PALEOGENE SECTIONS IN THE EASTERN RHODOPES (SE BULGARIA)

STILIYAN MOSKOVSKI[1], VASSIL KARLOUKOVSKI[2], ZLATKA MILAKOVSKA[3], ALEXANDRA HARKOVSKA[3] and MALCOLM PRINGLE[4]

[1]Faculty of Geology and Geography, Sofia University, Tzar Osvoboditel Bld. 15, 1500 Sofia, Bulgaria
[2]CEMP, Department of Geography, Lancaster University, Lancaster LA1 4YB, United Kingdom; v.karloukovski@lancs.ac.uk
[3]Geological Institute, Bulgarian Academy of Sciences, Acad. G. Bonchev Str. 24 Bl., 1113 Sofia, Bulgaria; zlatkam@geology.bas.bg, avhar@geology.bas.bg
[4]Manager, SURRC/NERC Argon Isotope Facility, Scottish Universities Research and Reactor Centre, Scottish Enterprise Technology Park, Rankine Avenue, East Kilbride G75 0QF, Scotland, United Kingdom; m.pringle@surrc.gla.ac.uk

(Manuscript received December 11, 2002; accepted in revised form October 2, 2003)

Abstract: Two multiple stratified volcano-sedimentary Paleogene sections built of breccia-conglomerates and sandstones (incl. epiclastic), marls, limestones (incl. reef and bioclastic) and zeolitized pyroclastic rocks (interpreted as pyroclastic flow deposits mainly) were studied and correlated. The deposits are divided into superposed and interfingered informal lithostratigraphic units. The natural remanent magnetization of the zeolitized pyroclastics was determined as thermal remanent magnetization (TRM) or partial TRM, and that of the sediments — as detrital remanent magnetization and post-detrital remanent magnetization. The characteristic remanent directions allowed straightforward construction of magnetostratigraphic profiles and yielded 12 reliable magnetic polarity zones and sequences of zones in the sections studied. The correlation of the sections was based on the magnetic polarity zones position, lithological features of the rocks and three $^{40}Ar/^{39}Ar$ age determinations of the zeolitized pyroclastics from different levels of the sections. The consistent (Rupelian — 32.28±0.07 to 31.82±0.07) ages plot entirely into the 12r polarity chron on the Geomagnetic Polarity Time Scale (GPTS) (Cande & Kent 1995). The data presented show that the polystage formation of the pyroclastic flows and the change of the contemporaneous sedimentation from clastic to biogenic took place in a relatively short time span of about 0.46 Ma.

Key words: Paleogene, Bulgaria, Eastern Rhodopes, correlation, lithology, magnetostratigraphy, $^{40}Ar/^{39}Ar$ age.

Introduction

During Late Eocene (Priabonian)–Oligocene the territory of South Bulgaria was affected by intensive processes of differential block movements, contemporaneous terrigenous (continental and marine) sedimentation and orogenic, collision related, magmatism (Dabovski et al. 1989). At the end of the Priabonian and during the Rupelian the Eastern Rhodopes were a complex archipelago in a vast shelf. Most of the islands were of volcanic origin. Apart from the tectonic regime, two groups of factors controlled their places, dimensions and shapes: a) polystage and polystyle activity of subaerial volcanoes composed of acid or/and intermediate volcanics and volcaniclastics and b) simultaneous (s.l.) processes of intensive catastrophic and erosional destruction of the volcanic edifices. The time and space combination of volcanic processes and marine sedimentation resulted in an accumulation of various clastic (incl. epiclastic), biogenic (incl. reef limestones), pyroclastic and diverse volcano-sedimentary deposits. In their relationships a dominating superposition is combined with complex interfingering and gradual lateral transition. Such lithological variability poses serious problems both from the litho- and chronostratigraphic points of view, which have not been solved satisfactorily on the basis of paleontological data only.

The aim of the investigations reported is to correlate two Eastern Rhodopes volcano-sedimentary sections using lithological, magnetostratigraphic and radiometric ($^{40}Ar/^{39}Ar$) methods.

Geological setting and lithology of the sections studied

Two multiple Paleogene sections (A and B) from the Momchilgrad-Arda magmatic region were studied ($\varphi = 41.5°$ N, $\lambda = 25.5°$ E). Section A is located to the west of Momchilgrad (Fig. 1) and consists of six segments situated: to the west-northwest of Sofiytsi, to the east of Vurhari, to the west and southwest of Gradinka, to the southwest of Sedlari, to the southeast of Slunchogled and to the east of Tyutyunche (the last lies outside the territory presented on Fig. 1). Section B is located to the southeast of Momchilgrad, consisting of four segments — to the west of Kos, to the southeast of Lale, to the north of Chayka and to the west-northwest of Karamfil (Fig. 2). The well stratified sedimentary (incl. epiclastic) and bed-

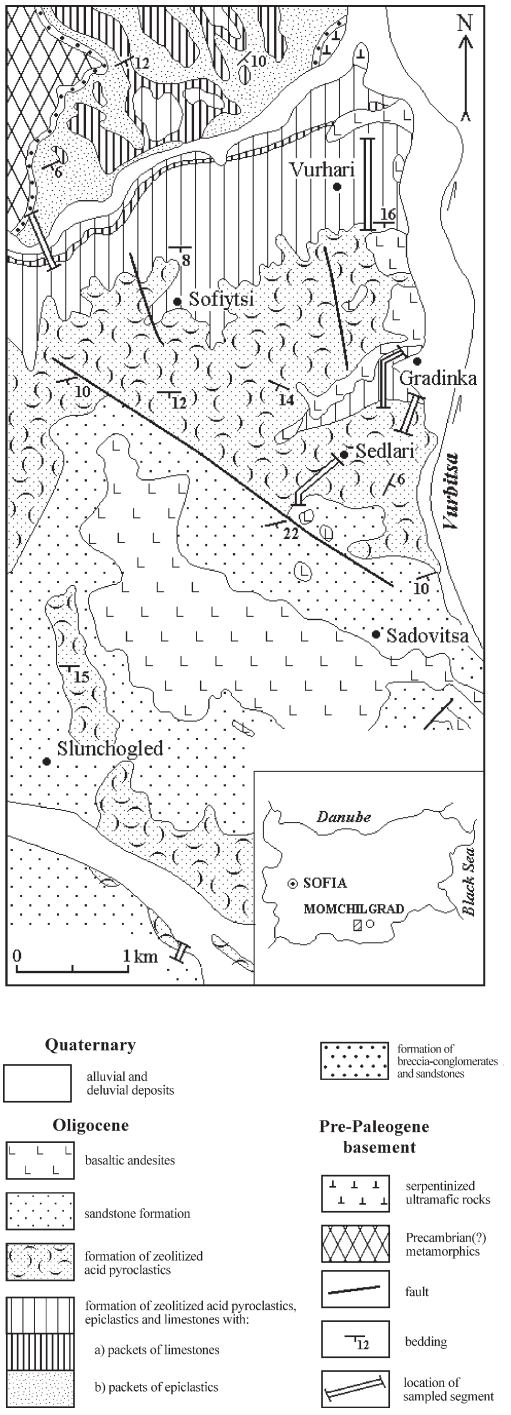

Fig. 1. Geological setting of the segments of the multiple section A (to the west of Momchilgrad). Segment Tyutyunche is located outside of the map. The map is according to Moskovski et al. (1990).

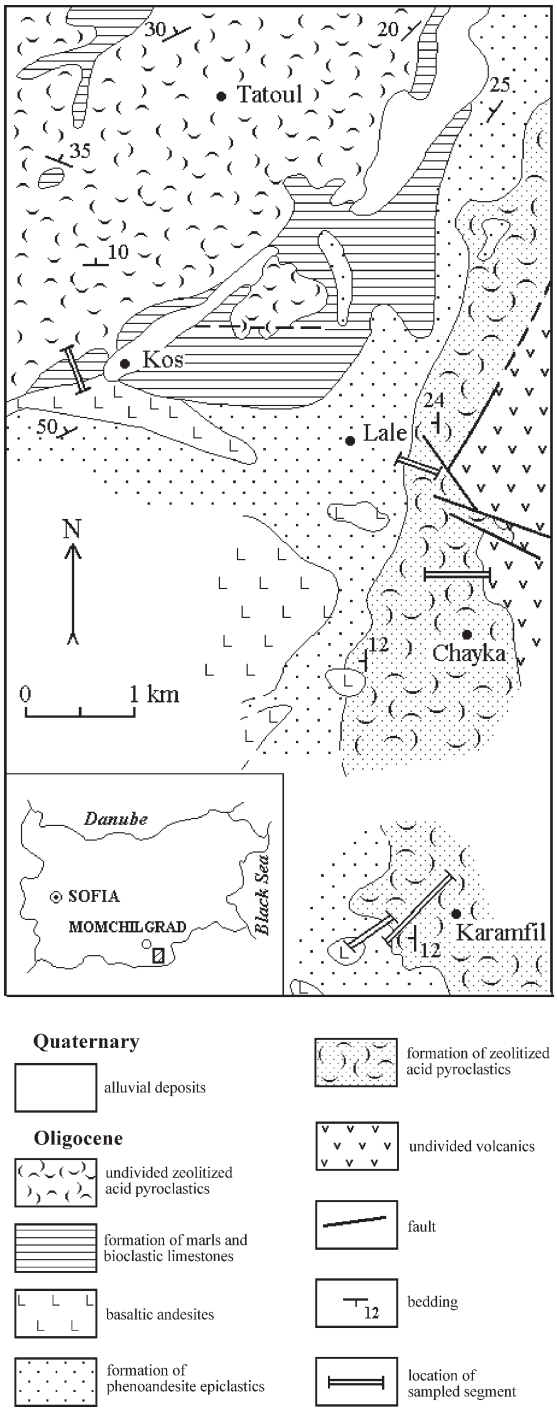

Fig. 2. Geological setting of the segments of the multiple section B (to the south-east of Momchilgrad). The map is according to Moskovski et al. (1990).

ded pyroclastic rocks cropping out along the sections are divided into six informal lithostratigraphic units:

Formation of breccia-conglomerates and sandstones

It overlays an uneven surface of Pre-Cambrian (?) gneisses and serpentinized ultramafic rocks (Fig. 1). The formation is built by polymict breccia-conglomerates and sandstones. The breccia-conglomerates (gravel- to cobble-size) are unsorted, with clasts from the basement's metamorphics mainly (gneisses, mica-schists, calc-silicate schists, marbles and metamorphic quartz). Well rounded clasts of serpentinized ultramafic rocks, polymict sandstones, polymict conglomerates and siltstones are rarely present. The sandstones are thick-bedded and

fine-grained. They are interbedded by thin siltstone layers. Their terrigenous component (quartz, feldspars and muscovite) is cemented by carbonate mineral.

The thickness of the formation varies from 0.4 to 25 m. Recently this formation was referred to the "conglomerate-sandstone packet" of the Oligocene "formation of the first acid volcanism" (Kozhoukharov et al. 1989).

Formation of zeolitized acid pyroclastics, epiclastics and limestones

It covers the previous formation nearly sharply (Fig. 1). The formation consists of an irregular alternation of zeolitized acid pyroclastics (former pyroclastic flows deposits) and packets of sedimentary rocks (sandstones, siltstones and limestones), containing epiclastic volcanic components in strongly variable quantities. The zeolitized pyroclastics are grey to white, grey-green, light green or grey-pink and are built mainly of former vitroclasts (Fig. 3). They also contain crystalloclasts of sanidine, acid plagioclase, biotite, cognate phenorhyolitic clasts and foreign clasts of phenoandesites and metamorphics. The thickness of the zeolitized pyroclastic packets varies from 10–12 to 65 m. The epiclastic sandstones and siltstones contain clasts of phenorhyolites, metamorphics and zeolitized pyroclastics, together with grains of acid plagioclase, hornblende, biotite, quartz and sanidine (Fig. 4). Rare bivalvian, foraminiferal, echinoidean, algal and bryozoan fragments are also present. The matrix is polymict, with calcite grains in some places. The limestones are micrite to biomicrite (acc. to the Folk's 1962 classification) or wackestones (acc. to the Embry & Klovan 1972 classification), sandy, with the epiclastic component dominating (Fig. 5).

The formation is about 150 m thick. On the geological map, scale 1:100,000 (Kozhoukharov et al. 1989) it is included into the Oligocene formations of "first acid volcanism" and of "second intermediate volcanism".

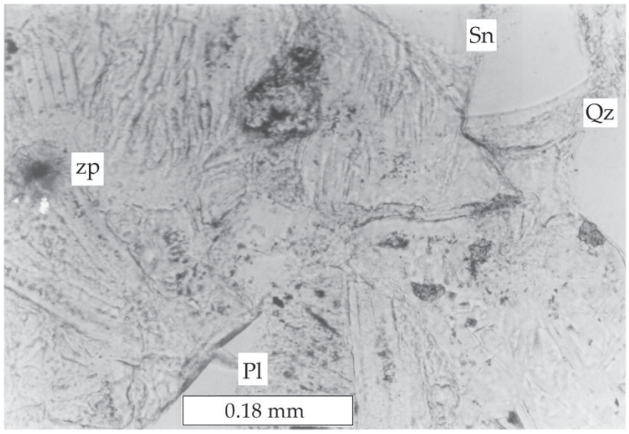

Fig. 3. Zeolitized acid pyroclastic rock: completely zeolitized pumices (**zp**), crystalloclasts of plagioclase (**Pl**), sanidine (**Sn**) and quartz (**Qz**). N ||. (Segment Sofiytsi, section A.)

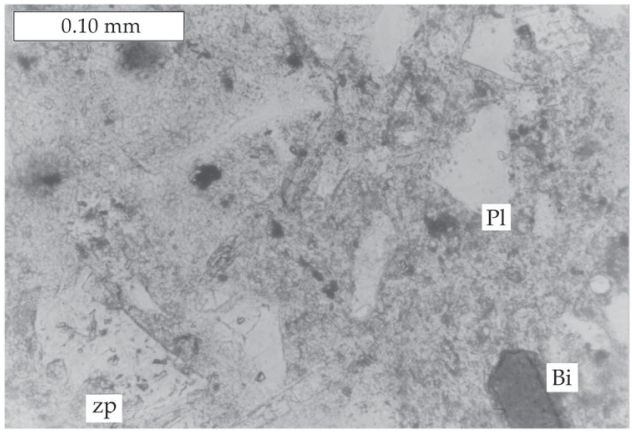

Fig. 4. Medium to fine epiclastic sandstone. Unrounded and unsorted grains of plagioclase (**Pl**), biotite (**Bi**) and zeolitized pumice fragments (**zp**) in microsparite groundmass. N ||. (Segment Gradinka, section A.)

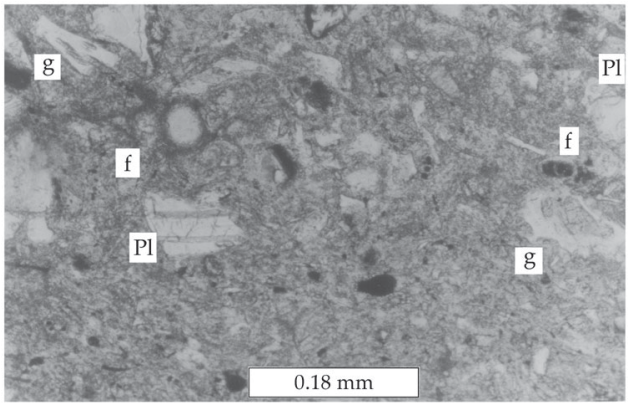

Fig. 5. Sandy fossiliferous microsparite limestone (wackestone). Unrounded and unsorted fresh clasts of plagioclase (**Pl**) and slightly altered glass shards (**g**). Biofragments of benthic and planktonic foraminifers (**f**). N ||. (Segment Sofiytsi, section A.)

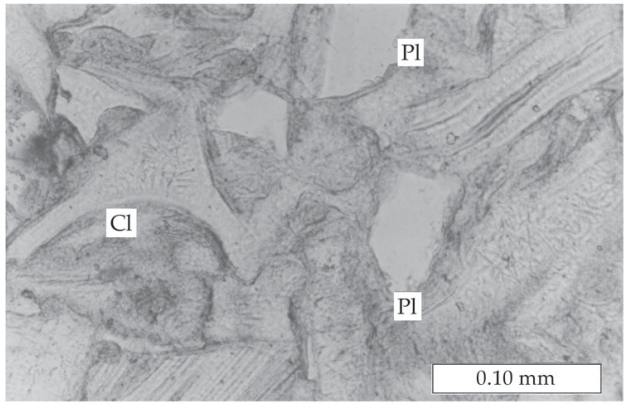

Fig. 6. Zeolitized acid pyroclastic flow deposit. The zeolitized glass shards and pumice fragments contact by clay (**Cl**) rim; crystalloclasts of plagioclase (**Pl**). N ||. (Segment Gradinka, section A.)

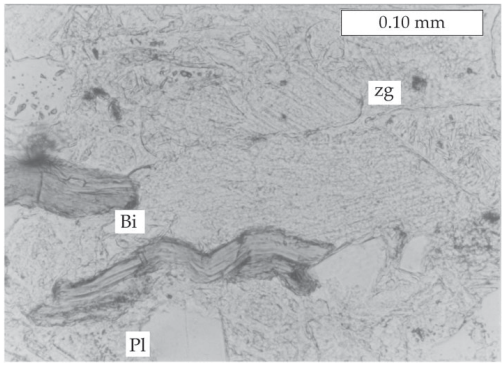

Fig. 7. Former pyroclastic flow deposit. Densely touched zeolitized glass fragments (**zg**), crystalloclasts of plagioclase (**Pl**) and deformed biotite (**Bi**). N ||. (Segment Slunchogled, section A.)

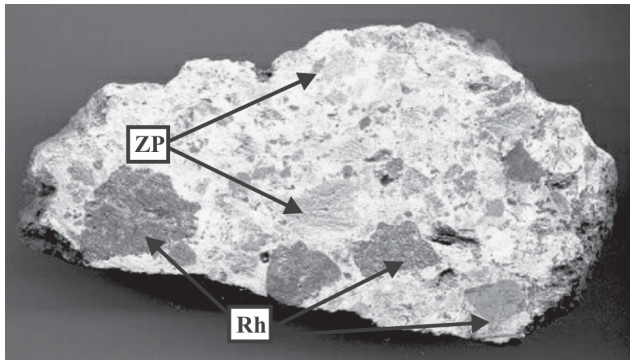

Fig. 8. Zeolitized pyroclastic flow deposit rich in cognate rhyolitic clasts (**Rh**) and zeolitized pumice fragments (**ZP**). The largest pumice is about 2.5 cm long. (Segment Chayka, section B.)

Formation of zeolitized acid pyroclastics

In section A (Fig. 1) it overlays the rocks of the previous formation conformably and with sharp contact. The zeolitized rocks (Boschinov 1976; Kirov et al. 1976) in that section are grey-white, thick-bedded to massive. They were formed as a result of alteration of ash-size pyroclastics mainly (Figs. 6, 7) and have a total thickness of about 90 m. It has to be noted that both their foreign volcanic clasts of intermediate composition and their acid cognate clasts contain early biotite, enclosed into pyroxene and plagioclase phenocrystals. This peculiarity is typical for the volcanics from the region of the Borovitsa caldera, located in the westernmost part of the Eastern Rhodope Paleogene magmatic area (unpublished data of P. Marchev in Moskovski et al. 1990). A genetic link between section A's former pyroclastics and the Borovitsa caldera activity was also suggested by Yanev (1995) and Raynov et al. (1997).

To the southeast of Momchilgrad (section B — Fig. 2) the formation was deposited above a series of undivided volcanics and volcaniclastics, which were not included into the sampling program. The zeolitized acid pyroclastics in that section are up to 140 m thick and are mainly composed of lapilli, to block varieties (Figs. 8, 9). Their primary pumice clasts and glass shards are completely replaced by zeolite minerals — clinoptilolite, mordenite, analcime (Djourova & Aleksiev 1984; Djourova & Boyadjiev 1999). The rocks of this formation are considered to be part of the "packet of rhyolitic and rhyodacitic tufaceous breccias, tuffs and tuffites" of the Oligocene "formation of the second acid volcanism" (Kozhoukharov et al. 1989, 1992).

Sandstone formation

It is known in the Bulgarian literature as "Djebel sandstones". The formation is presented in section A only (Fig. 1) where it overlays conformably the formation of the zeolitized acid pyroclastics. Their lowermost 10 m consist of grey-greenish epiclastic sandstones and siltstones, followed upward by quartz-feldspar sandstones, interbedded by sandy clays and siltstones (Bozhinov 1981). As a whole the rocks of the sandstone formation are loose and because of this only the lowermost 30 meters of their section were sampled for paleomagnetic studies. The lower level of the formation is referred to the Lower Oligocene on the basis of macrofauna assemblage (Sapoundjieva & Yanev 1984).

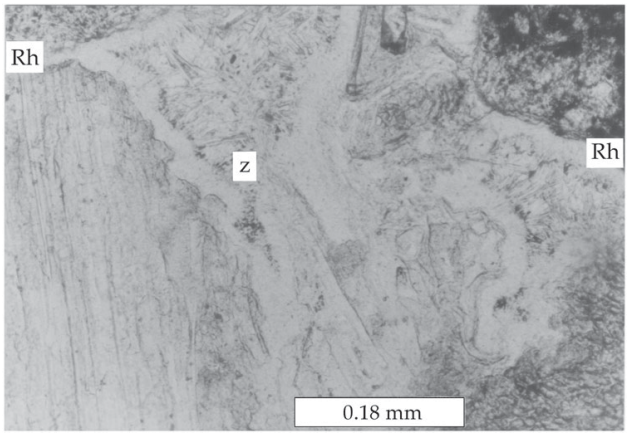

Fig. 9. Microphotograph of the sample of Fig. 8. The pores between the clasts are filled by zeolite crystals (**z**). N ||.

Fig. 10. Bedded epiclastic sandstones near Karamfil. (Segment Karamfil, section B.)

Formation of phenoandesite epiclastics (Moskovski et al. 1993; Harkovska et al. 1994)

This formation is presented in section B only. It overlays the formation of zeolitized pyroclastics (Fig. 2). Grey to yellowish thick bedded to massive sandstones and siltstones are the main rock types (Fig. 10). The sandstones from the lower levels of the formation pass upward into fine-grained sandstones and siltstones. In the upper levels the sandstones are interbedded with lenses of unsorted conglomerates with well-rounded pebble- and cobble-size clasts of intermediate volcanics (phenoandesites?). The presence of sparse small and undeformed pillows of intermediate to basic composition is another typical feature of the upper levels of this formation. Grains of acid plagioclase and clasts of phenorhyolites, rarely of phenoandesites, pyroxene and amphibole, are also distinguished as terrigenous components in the epiclastic sandstones (Fig. 11). Fragments of planktonic foraminifers and diatoms are also present. In some places the polymict matrix is replaced by calcite groundmass. The thickness of the formation is about 50 m. Some years ago the age of its lowermost levels was dated as Chattian (nannoplankton Zones NP24–NP25, Harkovska et al. 1998). On the geological map (scale 1:100,000) the rocks of the formation were referred to the Oligocene "formation of the third intermediate volcanism" (Kozhoukharov et al. 1992).

Formation of marls and bioclastic limestones (Moskovski et al. 1993)

This is a locally developed formation, which is presented in the section B only as a sequence overlaying the formation of phenoandesite epiclastics (Fig. 2). Dark grey sandy to silty fine-bedded marls are its main rock type. The marls are interbedded by lenses or thin beds of bioclastic limestones, sandstones and polymict conglomerates (Figs. 12, 13). This sedimentary sequence is about 65–75 m thick. On the recent geological map (scale 1:100,000) it is included in the "formation of the third intermediate volcanism" (Kozhoukharov et al. 1992). The paleontological age of the sequence is a controversial one: Priabonian — according to benthic foraminiferal assemblage (Harkovska et al. 1992) or Rupelian (unpublished nannoplankton determination of Kr. Stoykova). The undivided acid zeolitized pyroclastics, which crop out above this formation were not sampled for paleomagnetic studies, because they belong to a paleolandslide (Harkovska & Djourova 1994).

Magnetostratigraphy

A total of 434 oriented samples were collected from the 429 meters of section A and the 340 meters of section B, their positions marked as ticks to the right of the magnetic polarity profiles on Fig. 16. The average spacing between sampling levels was 2.2 m (section A) and 2.3 m (section B). The samples were divided into three main groups: a) zeolitized acid pyroclastics; b) epiclastic sandstones and siltstones; and c) marls and bioclastic limestones. Their natural remanent mag-

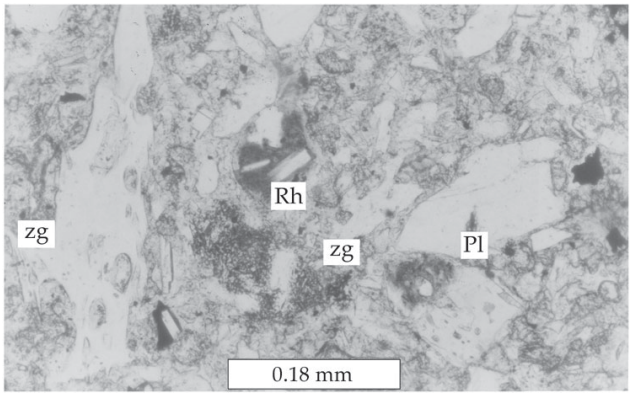

Fig. 11. Coarse to medium epiclastic sandstone. Unsorted and unrounded clasts of plagioclase (**Pl**), phenorhyolite (**Rh**) and zeolitized glass (**zg**). The matrix is polymict, partially replaced by microsparite. N ||. (Segment Karamfil, section B.)

Fig. 12. Alternation of marls and bioclastic limestones in segment Kos (section B).

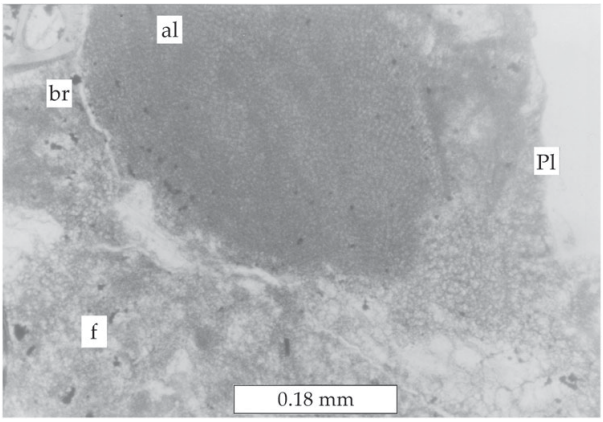

Fig. 13. Biomicrite limestone (wackestone to packstone) with bryozoan (**br**), algal (**al**) and foraminiferal (**f**) biofragments and rare plagioclase (**Pl**) clasts. N ||. (Segment Kos, section B.)

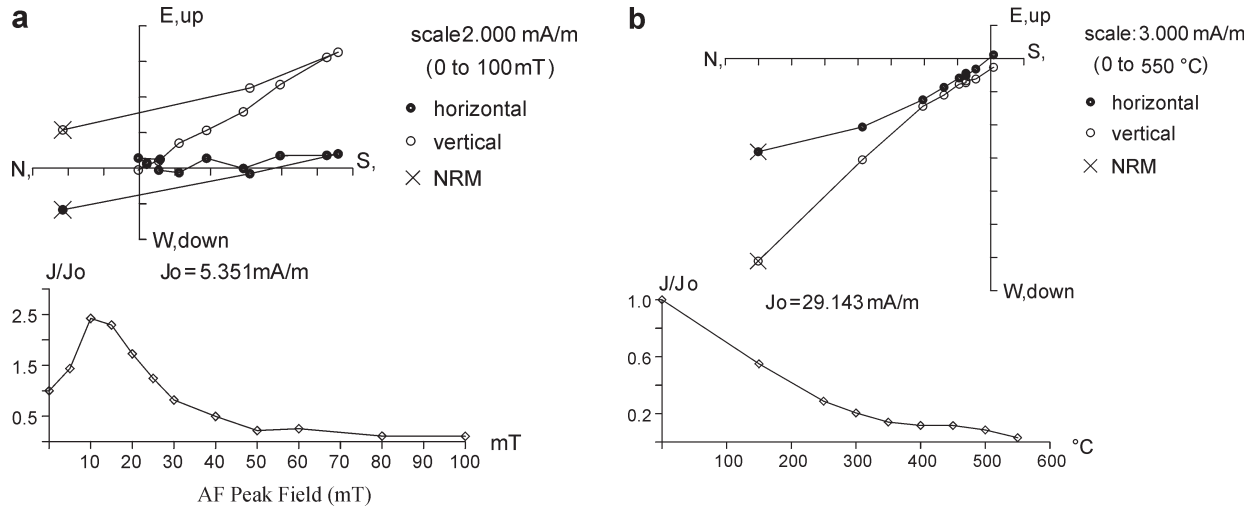

Fig. 14. Typical AF (**a**) and thermal (**b**) demagnetization characteristics of NRM. Zeolitized acid pyroclastics (sample D261, segment Sedlari, section A) were used in (a), and epiclastic sandstones (sample D291, segment Vurhari, section A) — in (b).

netization (NRM) was measured at the School of Environmental Sciences, University of East Anglia (Norwich) with spinner and cryogenic magnetometers. On the basis of their relatively high Koenigsberg ratios Q_n (average $Q_n = 0.95$), the NRM of the first group was most probably a thermoremanence (TRM) or, as in the case of the pyroclastics from segments Karamfil, Lale and Chayka, which contain abundant foreign clasts — a partial TRM. Alternating field (AF) demagnetizations of these pyroclastics were completely chaotic, while the thermal ones revealed linearity up to a certain point only — the point of the emplacement temperature. With average Q_ns of 0.43 and 0.24, respectively, the NRM of the epiclastic rocks, marls and limestones was detrital (DRM) or post-detrital (PDRM).

A strong viscous overprint of normal polarity was frequently revealed in stepwise AF or high-temperature demagnetization in all rocks. It was cleaned after 200–250 °C or 20–25 mT AF field (Fig. 14a), after which point straight linear segments on the Zijderveld plots (Zijderveld 1967) determined unambiguously characteristic remanent magnetization (ChRM) directions of either normal or reversed polarity. The sample's ChRM directions were predominantly normal or reversed. In single cases, transitional polarities were isolated, and these were excluded from the analysis. The thermal demagnetization of the NRMs and of three-component isothermal remanent magnetization (Lowrie 1990) revealed two main unblocking temperatures — one, around 300–400 °C, corresponding to medium titanomagnetites (TM30–TM40) (Heller et al. 1979), and a second, magnetite-like temperature of 550–570 °C (Fig. 14b).

Hysteresis measurements in fields up to 1 T on a vibrating sample magnetometer, modified to additionally measure back-field curves, identified predominantly multidomain (MD) and some pseudo-single domain (PSD) carriers of remanence in the zeolitized acid pyroclastics ($J_{rs}/J_s = 0.03–0.2$, $H_{cr}/H_c = 2.5–12$) (Day et al. 1977). The sedimentary rocks were magnetically harder, with mainly PSD and some MD medium titanomagnetites and magnetites ($J_{rs}/J_s = 0.04–0.3$, $H_{cr}/H_c = 2–8$).

The demagnetization characteristics of 125 (29 %) of all pyroclastic and sediment samples were of quality (linearity, number of demagnetization points and span of the segment used to calculate the ChRM) high enough to be comparable to that of the intermediate and acid volcanic bodies from the area between sections A and B studied alongside them (Karloukovski 2000). These pyroclastic and sediment samples came from four segments to the west of Momchilgrad and from one segment — to the east of Momchilgrad. Their site-averaged ChRM directions are given in Table 1 and are plotted on Fig. 15. The mean positive and the mean negative ChRM directions ($D = 6.5°$, $I = 54.8°$, $\alpha_{95} = 14.4°$ and $D = 182.7°$, $I = -53.3°$, $\alpha_{95} = 9.7°$ correspondingly) pass McFadden & Elhinney's (1990) reversal test and are essentially antipodal (Karloukovski 2000). The antipodality is an important indicator of the adequate removal of secondary overprints and of the primary nature of the isolated ChRMs, especially in view of the closeness of the mean positive ChRM direction to the modern axial dipole field for the area ($D = 0°$, $I = 60.5°$) (Fig. 15). The mean ChRM direction from all sediments and pyroclastics ($D = 184.5°$, $I = -54.1°$, $\alpha_{95} = 7.0°$) is close to the mean direction

Table 1: Site mean directions in the pyroclastics and the sediments. Segment Lulichka is located to the south of Karamfil (Fig. 2), outside the map. N — number of samples; D, I — site mean declination and inclination; α_{95} — confidence limit.

Segment	N	D (°)	I (°)	α_{95} (°)
Kos (marls, limestones)	14	0.1	39.7	10.8
Lulichka (marls, limestones)	6	18.1	47.3	13.9
Sedlari (pyroclastics)	13	171.4	–50.6	9.5
Vurhari, negative (pyroclastics)	22	178.3	–52.2	19.5
Vurhari, positive (pyroclastics)	5	7.1	64.4	14.3
Gradinka, negative (pyroclastics)	44	189.5	–54.4	4.5
Gradinka, positive (pyroclastics)	21	4.6	62.5	6.4
Mean (negative)	**3**	**182.7**	**–53.3**	9.7
Mean (positive)	**4**	**6.5**	**54.8**	14.4
Mean (all)	**7**	**184.5**	**–54.1**	7.0

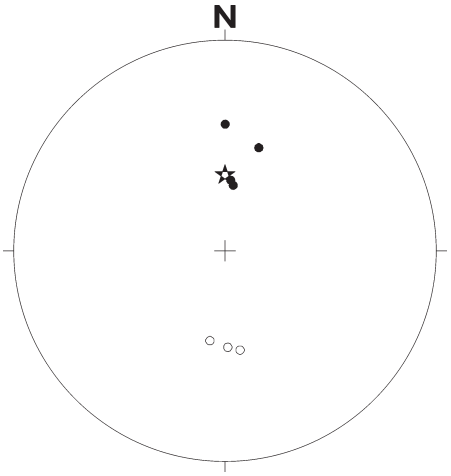

Fig. 15. Stereoplot of the site-mean directions in the sediments and pyroclastics. The star indicates the direction of the present dipole magnetic field. Open and closed symbols denote the lower and upper hemisphere projections, correspondingly.

(D = 182.9°, I = –51.4°, α_{95} = 5.2°, 12 sites) obtained from the neighbouring lava rocks (Karloukovski 2000). This would suggest a PDRM rather than a DRM origin of the NRMs in the sediments due to the lack of inclination shallowing.

The magnetic polarity section between the radiometric data (32.28 to 31.82 Ma) includes at least 7 polarity events, five of which (N4 to N6, N8 and N9) are securely attested in multiple sections. Some of them, like N6, are most certainly polarity excursions and could not have been registered on the GPTS. Others are 10 to 20 meters high (N4, N8 — in sediments) and probably 10 to 20 ka in duration. We think that some of them correspond to the three registered cryptochrons of normal polarity in the 12r chron — C12r-5, C12r-4, C12r-3 (Cande & Kent 1995).

The ChRM directions of the sediments and pyroclastics allowed straightforward construction of the magnetostratigraphic profiles, and yielded reliable magnetic polarity zones and sequences of zones in the two multiple sections studied (the normal zones being numbered through N1 to N12 from bottom to top) (Fig. 16).

Radiometric data

Three samples of zeolitized acid pyroclastic rocks from the both sections studied were crushed, sieved and passed through Franz separator, before single crystals of sanidine and biotite could be hand-picked. The samples were analysed at SURRC in East Kilbride, UK using a mass spectrometer and gas line devoted to low radiogenic argon content rocks. Step-heating experiments were combined with single-crystal fusion analyses for best total average age. Analytical procedures were similar to those used by Singer et al. (1999). The samples, along with 27.92 Ma sanidine standard Tcr-2a, were placed in quartz vials and irradiated at the Oregon State University Triga reactor in the cadmium lined in-core irradiation tube (CLICIT). Prior to the analyses, samples were degassed in a vacuum for approximately 2 weeks to remove any absorbed air. To release the radiogenic and potassium-derived argon, individual samples were heated to progressively higher temperatures in a double vacuum furnace from around 500 to 1200 °C over 9–12 steps. Reactive gases were removed using a two-stage gas clean up, incorporating hot (450 °C) and cold (room temperature) ZrAl getters. A zeolite cold finger was used to trap hydrocarbons. Relative amounts of the different argon isotopes in the cleaned gas fraction were measured with a MAP-215 spectrometer. The $^{40}Ar/^{39}Ar$ ratios used to calculate the age for each step were corrected for Ca-derived ^{39}Ar, air-derived ^{40}Ar, the equipment blank and mass spectrometer mass discrimination. The analytical errors of all these quantities were included in the standard deviation. Criteria for selecting reliable results have been established by Singer & Pringle (1996).

All the three ages obtained plot onto the Rupelian time span of the Gradstein & Ogg's (1996) timescale — Table 2.

Correlations

The following correlations of the sections studied could be made using the data reported:

1. The specific alternation of the normal polarity zones from N7 to N9 (Fig. 16), revealed in the both sections, led to their secure leveling (Karloukovski 2000) and could be used as a marker in the magnetostratigraphic correlations:

a) The lowermost levels of the sandstone formation in section A (epiclastic rocks in segments Tyutyunche and Slunchogled) and the lowermost levels of the formation of phenoandesite epiclastics in section B (segment Karamfil) have to be correlated because they belong to the N8 polarity zone. These levels are also very well comparable from the lithological point of view.

b) The uppermost 40 m of the formation of zeolitized acid pyroclastics in section A and the whole 140 m of the same formation in section B have to be correlated not only on the basis of the magnetostratigraphic data (both intervals belong

Table 2: $^{40}Ar/^{39}Ar$ ages of zeolitized acid pyroclastics.

Sample Number	Mineral	Number of crystals	Number of analyses	Age (Ma)	σ (Ma)	Section and segment	Geological age according to Gradstein & Ogg (1996)
D337	Sanidine	6	15	32.28	±0.07	A, Vurhari	Rupelian
D227	Sanidine	6	10	32.00	±0.06	A, Sedlari	Rupelian
D462	Biotite	6	6	31.82	±0.07	B, Karamfil	Rupelian

σ — standard deviation of the normal distribution

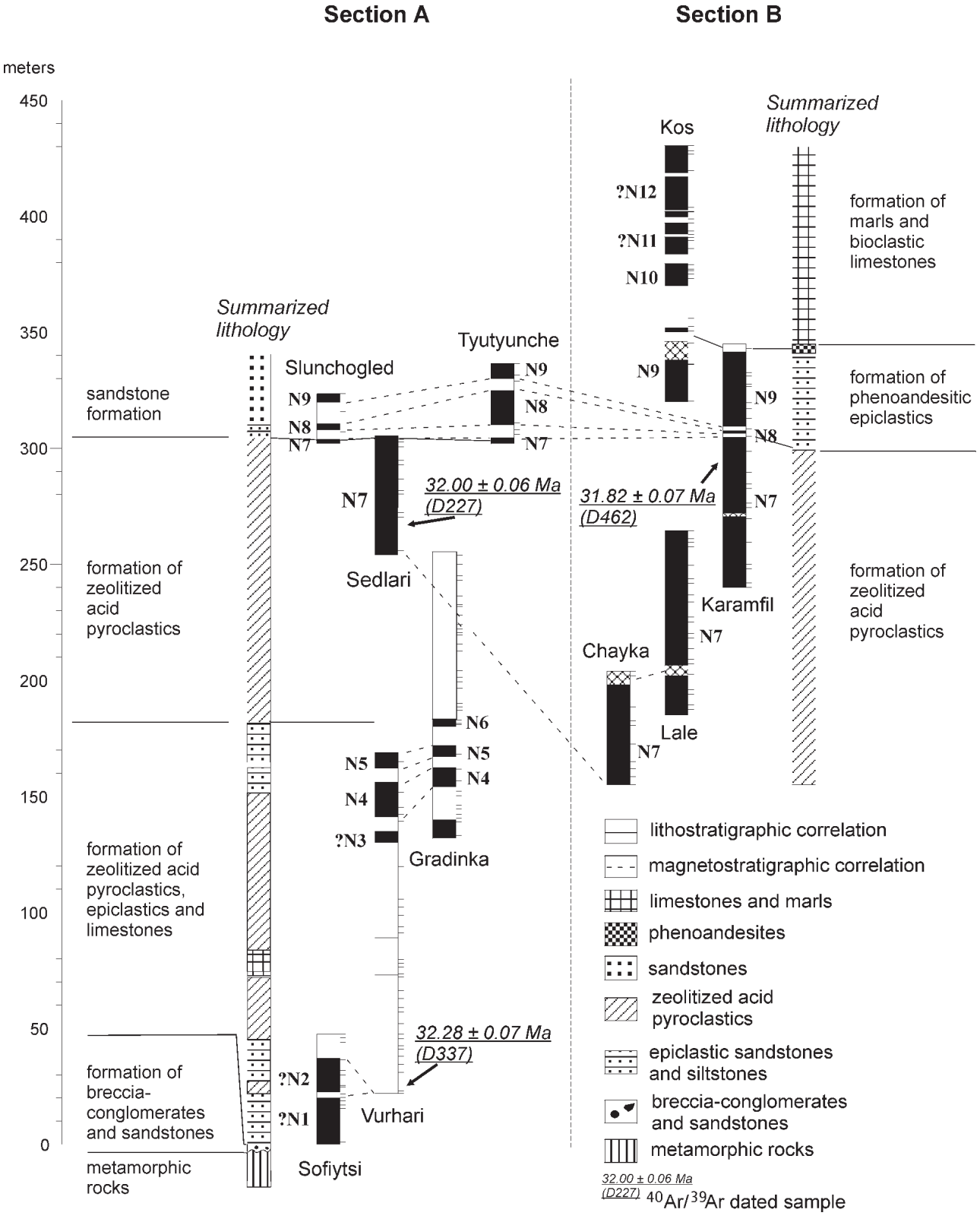

Fig. 16. Magnetostratigraphy and proposed correlation of the sections studied. The normal polarity zones on the magnetostratigraphic columns are shown in black and are numbered from N1 to N12, the reverse ones — in white, the transitional zones are hatched.

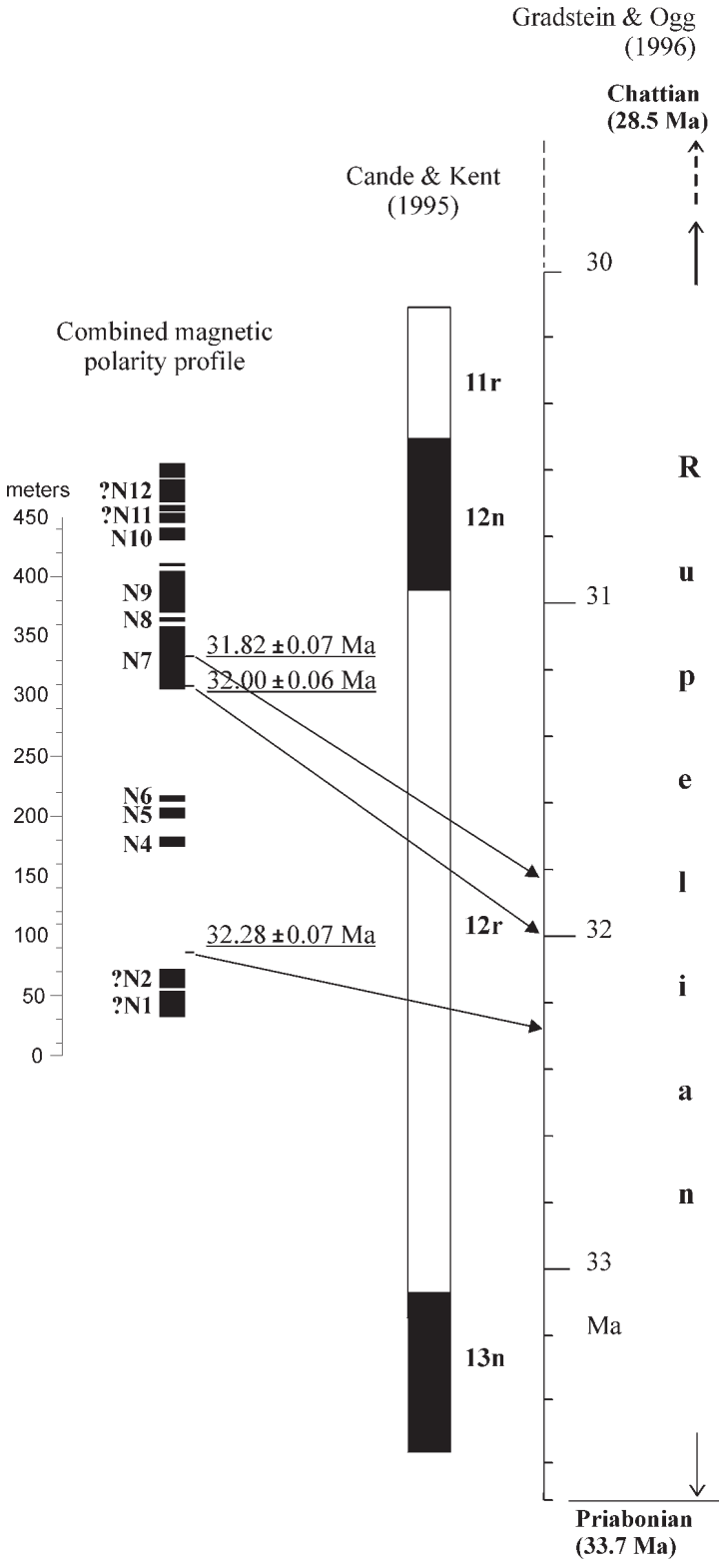

Fig. 17. Position of the combined magnetic polarity profile of the sections studied on the Geomagnetic Polarity Time Scale (Cande & Kent 1995) and on the Geological Timescale of Gradstein & Ogg (1996).

to the N7 polarity zone), but according to their $^{40}Ar/^{39}Ar$ ages and lithological features as well.

2. On the Geomagnetic Polarity Time Scale (GPTS) the dated part of section A (between samples D337 and D227), which corresponds to a time span of 0.46 Ma, falls entirely within the lower part of the 12r polarity chron (Fig. 17). This result is in agreement with the paleomagnetic data on previously studied volcanic bodies from a territory situated between the sections studied (Dolapchieva et al. 1986).

3. The $^{40}Ar/^{39}Ar$ age of biotite (31.8 ± 0.07 Ma — Sp. No. D462, segment Karamfil, section B; Table 2) is consistent with the $^{40}Ar/^{39}Ar$ age of plagioclase (31.39 ± 0.50 Ma) from similar pyroclastics near Karamfil (Singer & Marchev 2000). The cited authors interpreted these pyroclastics as "outflow tuffs" of the Borovitsa caldera. The same origin could be suggested for all the zeolitized pyroclastic flows deposits in section A, having in mind their age and the common petrographic features of their foreign and cognate clasts on one hand and the intermediate and acid volcanics from the Borovitsa volcanic region — on the other.

4. The differences in the dimensions of the former pyroclasts and cognate clasts in the zeolitized acid pyroclastics in section A as compared with those in section B could be explained with a suggestion that the respective pyroclastic flow deposits were related to different explosive events in the Borovitsa caldera realm.

Conclusions

1. The study shows that the combination of lithostratigraphic, magnetostratigraphic and high-resolution radiometric ($^{40}Ar/^{39}Ar$) data can be a very useful tool for correlation of complex stratified volcano-sedimentary sections and for discrimination of the respective volcanic events and processes:

a) Two lithostratigraphic units of different lithology (sandstone formation — section A and formation of epiclastics — section B) were completely correlated.

b) Two lithostratigraphic units of completely comparable lithology (formation of zeolitized acid pyroclastics) were partially only correlated.

2. The polystage formation of pyroclastic flows, their zeolitization into the Rupelian marine basin and the contemporaneous sedimentation took place in a relatively short time span of approximately 0.46 Ma, as is shown by the $^{40}Ar/^{39}Ar$ dating of different levels of section A.

3. The accumulation of the rocks in the area of section A is a result of sedimentation and contemporaneous acid explosive volcanic activity in the Borovitsa caldera realm. Volcanic products related to centre(s) of intermediate composition (mentioned by many previous authors) were not recorded in the territory in question.

Acknowledgments: The paleomagnetic and $^{40}Ar/^{39}Ar$ studies were financed by Lord Zuckermann's studentship at the University of East Anglia, Norwich. The geological maps (Fig. 1 and Fig. 2) are from the report of the Project 16604-K (Subproject 2), Sofia University. The authors would like to express their gratitude to the reviewers Dr. N. Yordanova, Dr. A. Di Stefano and Dr. I. Túnyi for the critical and helpful comments. Y. Zagorcheva drew figures 1 and 2.

This paper was presented at the XVIIth Congress of Carpathian-Balkan Geological Association held in Bratislava, SR, in September 2002.

References

Boschinov K. 1976: Über die Ausdehnung und über die mineralchemische Charakteristik einer Schicht Öligozänisch-vulkanischer Tuffe von den Südöstlichen Rhodopen. *Ann. de l'Univ. de Sofia "Kl. Ohridski", Ser. 1 — Geol.* 68, 1, 279–288 (in Bulgarian, German abstract).

Bozhinov K. 1981: Composition of the Djebel sandstones. *Rev. Bulg. Geol. Soc*. 42, 1, 130–137 (in Bulgarian).

Cande S. & Kent D. 1995: Revised calibration of the geomagnetic polarity time scale for the Late Cretaceous and Cenozoic. *J. Geophys. Res*. 100, 6093–6095.

Dabovski C., Harkovska A., Kamenov B., Mavroudchiev B., Stanisheva-Vassileva G. & Yanev Y. 1989: Geodynamic model of the Alpine magmatism in Bulgaria. *XIV Congress CBGA. Reports,* Sofia, 44–66.

Day R., Fuller M. & Schmidt V. 1977: Hysteresis properties of titanomagnetites: grain size and compositional dependence. *Phys. Earth Planet. Inter.* 13, 260–267.

Djourova E. & Aleksiev B. 1984: Zeolitic rocks deposits of economic value in the North-Eastern Rhodopes. *Ann. de l'Univ. de Sofia "Kl. Ohridski", L. 1 — Geol.* 78, 256–262 (in Bulgarian, English abstract).

Djourova E. & Boyadjiev S. 1999: The zeolitic rocks in the vicinity of Karamfil village, Haskovo district — mineralopetrographic and geochemical characteristics. *Geology and Mineral Resources* 7, 18–23 (in Bulgarian, English abstract).

Dolapchieva M., Nozharov P. & Petkov N. 1986: Paleomagnetic characteristics of the young volcanics of the Eastern-Rhodopean depression. *Bulg. Geophysical J*. 12, 2, 114–126 (in Bulgarian, English abstract).

Embry E. & Klovan J. 1972: Absolute water depth limits of late Devonian paleoecological zones. *Geol. Rdsch.* 61, 672–686.

Folk R. 1962: Spectral subdivision of limestone types. In: Ham W.E. (Ed.): Classification of carbonate rocks. *Amer. Assoc. Petrol. Geol. Mem*. 1, 62–84.

Gradstein F. & Ogg J. 1996: Geological timescale. *Episodes* 19, 1–2.

Harkovska A. & Djourova E. 1994: Petrologic features and slump redeposition of Paleogene rhyolitic tuffs from Eastern Rhodopes (Bulgaria). *Int. Volcanol. Congr. IAVCEI 1994*, Ankara, Abstracts, 1–69.

Harkovska A., Moskovski S. & Jouranov S. 1992: Upper Eocene (Priabonian) rhyolite tuffs in the region of Dambaluk Mountain (East Rhodopes, Bulgaria). *Geol. Balcanica* 22, 1, 74.

Harkovska A., Moskovski S. & Nedyalkov R. 1994: Paleogene volcanomictic sediments (epiclastics) in the south-eastern parts of the Momchilgrad-Ardino volcanic region (SE Bulgaria). *C. R. Acad. Bulg. Sci*. 47, 10, 53–56.

Harkovska A., Pe-Piper G., Stoykova K., Nedyalkov R. & Moskovski S. 1998: Late Oligocene (Chattian) epiclastics and lava flows of intermediate composition from the Eastern Rhodopes (Bulgaria). *C. R. Acad. Bulg. Sci*. 51, 7–8, 53–58.

Heller F., Markert H. & Schmidtbauer E. 1979: Partial self-reversal of NRM of an historical lava flow of Mt. Etna (Sicily). *J. Geophys.* 45, 235–257.

Karloukovski V. 2000: Magnetostratigraphy and palaeomagnetism of the area around the Momchilgrad Paleogene depression, the East Rhodope massif. *PhD Thesis*, University of East Anglia, Norwich, 1–343.

Kirov G., Pechigargov V. & Chelebiev E. 1976: Effect of the grain size of volcanic glass on the mineral composition of its alteration products. *Geochemistry, Mineralogy and Petrology,* 4, 83–90 (in Bulgarian, English abstract).

Kozhoukharov D., Boyanov I., Goranov A., Yanev Y., Shilyafova J. & Rousseva M. 1989: Geological map of Bulgaria, Scale 1:100,000, Sheet Kurdjali, Sofia.

Kozhoukharov D., Boyanov I., Goranov A. & Kozhoukharova E. 1992: Geological map of Bulgaria, Scale 1:100,000, Sheet Kroumovgrad and Sape, Sofia.

Lowrie W. 1990: Identification of ferromagnetic minerals in a rock by coercivity and unblocking temperature properties. *Geophys. Res. Lett*. 17, 159–162.

McFadden P. & McElhinny M. 1990: Classification of the reversal test in paleomagnetism. *Geophys. J. Int.* 103, 725–729.

Moskovski S., Harkovska A. & Marchev P. 1993: New data on the stratigraphy of the Paleogene in the Dambaluk volcanic massif. *C. R. Acad. Bulg. Sci*. 46, 6, 61–64.

Moskovski S., Harkovska A., Marchev P., Jouranov S. & Lilov P. 1990: Stratigraphic, petrologic and structural-volcanologic studies in the Dambaluk volcanic massif. Project 16604-K, Subproject 2. *Fac. of Geol. and Geogr., Sofia University,* Sofia (in Bulgarian, unpublished).

Raynov N., Popov N., Yanev Y., Petrova P., Popova T., Hristova V., Atanasova R. & Zankarska R. 1997: Geological, mineralogical and technological characteristics of zeolitized (clinoptilolitized) tuff deposits in the Eastern Rhodopes, Bulgaria. In: Kirov G., Filizova L. & Petrov O. (Eds.): Natural zeolites. Sofia'95. *PENSOFT*, Sofia–Moscow, 263–275.

Sapoundjieva V. & Yanev Y. 1984: Fauna from the sandstones near Djebel, East Rhodopes. *Rev. Bulg. Geol. Soc*. 45, 308–317 (in Bulgarian, English abstract).

Singer B. & Marchev P. 2000: Temporal evolution of arc magmatism and hydrothermal activity, including epithermal gold veins, Borovitsa caldera, Southern Bulgaria. *Econ. Geol.* 95, 1155–1164.

Singer B., Hoffman K., Chauvin A., Coe R. & Pringle M. 1999: Dating transitionally magnetised lavas of the late Matuyama Chron: toward a new $^{40}Ar/^{39}Ar$ timescale of reversals and events. *J. Geophys. Res*. 104, 679–693.

Singer B. & Pringle M. 1996: Age and duration of the Matuyama–Brunhes geomagnetic polarity reversal event from $^{40}Ar/^{39}Ar$ incremental heating analyses of lavas. *Earth Planet. Sci. Lett*. 139, 47–61.

Yanev Y. 1995: General characteristics of the Late Paleogene collision volcanism in the Rhodopes. In: Aleksiev B. (Ed.): Sofia Zeolite Meeting '95, International Symposium and Exhibition on Natural Zeolites, June 18–25, 1995, Sofia, Bulgaria. *Guide to the Post-Meeting Field Trip,* 3–19.

Zijderveld J. 1967: A.C. demagnetization of rocks: Analysis of results. In: Collinson D., Creer K. & Runcorn S. (Eds.): Methods in palaeomagnetism. *Elsevier,* Amsterdam, 254–286.